

Tunable polaritonic molecules in an open microcavity system

S. Dufferwiel, Feng Li, A. A. P. Trichet, L. Giriunas, P. M. Walker, I. Farrer, D. A. Ritchie, J. M. Smith, M. S. Skolnick, and D. N. Krizhanovskii

Citation: [Applied Physics Letters](#) **107**, 201106 (2015); doi: 10.1063/1.4936092

View online: <http://dx.doi.org/10.1063/1.4936092>

View Table of Contents: <http://scitation.aip.org/content/aip/journal/apl/107/20?ver=pdfcov>

Published by the [AIP Publishing](#)

Articles you may be interested in

[Strong exciton-photon coupling in open semiconductor microcavities](#)

Appl. Phys. Lett. **104**, 192107 (2014); 10.1063/1.4878504

[Effect of magnetic field on polariton emission characteristics of a quantum-well microcavity diode](#)

Appl. Phys. Lett. **100**, 171106 (2012); 10.1063/1.4707155

[Estimating the conditions for polariton condensation in organic thin-film microcavities](#)

J. Chem. Phys. **136**, 034510 (2012); 10.1063/1.3678015

[Boundary effects on the dynamics of exciton polaritons in semiconductor microcavities](#)

J. Appl. Phys. **105**, 033105 (2009); 10.1063/1.3075908

[Polariton quantum boxes in semiconductor microcavities](#)

Appl. Phys. Lett. **88**, 061105 (2006); 10.1063/1.2172409

The advertisement for MMR Technologies features a blue and white background with a grid pattern. On the left is the MMR Technologies logo, which consists of the letters 'MMR' in a bold, sans-serif font, with 'TECHNOLOGIES' in a smaller font below it, all enclosed in a stylized blue and white oval. To the right of the logo, the text 'THE WORLD'S RESOURCE FOR VARIABLE TEMPERATURE SOLID STATE CHARACTERIZATION' is displayed in a bold, black, sans-serif font. Below this text, there are five images of different scientific instruments: a small white box, a blue box labeled 'SB1000', a blue box labeled 'K2000', a white circular device, and a blue box labeled 'H2000'. To the right of these images is a large, complex piece of equipment with multiple coils and a central column. At the bottom of the advertisement, the website 'WWW.MMR-TECH.COM' is written in a bold, red, sans-serif font. Below the website, there are five labels: 'OPTICAL STUDIES SYSTEMS', 'SEEBECK STUDIES SYSTEMS', 'MICROPROBE STATIONS', 'HALL EFFECT STUDY SYSTEMS AND MAGNETS', and 'HALL EFFECT STUDY SYSTEMS AND MAGNETS'.

Tunable polaritonic molecules in an open microcavity system

S. Dufferwiel,¹ Feng Li,^{1,a)} A. A. P. Trichet,² L. Giriunas,¹ P. M. Walker,¹ I. Farrer,³ D. A. Ritchie,³ J. M. Smith,² M. S. Skolnick,¹ and D. N. Krizhanovskii^{1,b)}

¹Department of Physics and Astronomy, University of Sheffield, Sheffield S3 7RH, United Kingdom

²Department of Materials, University of Oxford, Oxford OX1 3PH, United Kingdom

³Cavendish Laboratory, University of Cambridge, Cambridge CB3 0HE, United Kingdom

(Received 24 August 2015; accepted 6 November 2015; published online 17 November 2015)

We experimentally demonstrate tunable coupled cavities based upon open access zero-dimensional hemispherical microcavities. The modes of the photonic molecules are strongly coupled with quantum well excitons forming a system of tunable polaritonic molecules. The cavity-cavity coupling strength, which is determined by the degree of modal overlap, is controlled through the fabricated centre-to-centre distance and tuned *in-situ* through manipulation of both the exciton-photon and cavity-cavity detunings by using nanopositioners to vary the mirror separation and angle between them. We demonstrate micron sized confinement combined with high photonic Q-factors of 31 000 and lower polariton linewidths of 150 μeV at resonance along with cavity-cavity coupling strengths between 2.5 meV and 60 μeV for the ground cavity state. © 2015 AIP Publishing LLC.

[<http://dx.doi.org/10.1063/1.4936092>]

Photonic molecules are two or more coupled electromagnetically interacting microcavities. In the most simple case, two zero-dimensional microcavities are brought together so that their photonic modes interact, leading to hybridisation and the formation of bonding (B) and anti-bonding (AB) modes with an energy splitting given by the coupling strength, J . The initial demonstrations of lithographically fabricated photonic molecules coupled two adjacent cavities leading to a direct analogy with a simple diatomic molecule.^{1,2} Alternative configurations of photonic molecules exist such as square-shaped photonic dots coupled via a semiconductor bridge;¹ coupled defects in photonic crystal membranes;³ whispering-gallery microdisks coupled via a small air gap;⁴ and planar Fabry-Perot cavities coupled through a partially transparent distributed Bragg reflector (DBR).⁵ More complicated structures such as photonic graphene have been developed where a honeycomb lattice of coupled micropillars displays polariton dispersions which are analogous to the electronic bandstructure of its chemical counterpart.⁶ Coupled micropillars have found applications in the development of ultrabright entangled photon sources⁷ along with Josephson oscillations between two linked polariton condensates.⁸ Recent theoretical proposals have shown that a weak nonlinearity in a coupled cavity system can lead to a strongly antibunched single photon source in a process termed unconventional polariton blockade.^{9–11} A coupled cavity system based upon coupled micropillars containing quantum wells (QWs) is likely to be unsuitable to observe this effect since the etching required to achieve micron sized lateral confinement, and hence enhance the nonlinear polariton-polariton interaction to practical values, leads to significant degradation of the polariton linewidth.¹² Consequently, to experimentally demonstrate this blockade effect in III-V QW systems an alternative coupled cavity system which can concurrently achieve narrow polariton

linewidths, strong lateral confinement, and controllable cavity tunneling times is required.

In this study, we demonstrate a suitable coupled cavity system based upon spectrally tunable open access polaritonic molecules. The system is formed through reducing the centre-to-centre distance between adjacent zero-dimensional cavities during mirror fabrication so that hybridisation of the modal structure occurs. The cavity resonances of the coupled cavity system are strongly coupled to QW excitons, present in a cavity region above the bottom semiconductor DBR, giving rise to hybrid light-matter eigenstates and the formation of a polaritonic molecule. *In-situ* manipulation of both the exciton-photon detuning and cavity-cavity detuning using nanopositioners allows full control over the cavity-cavity coupling strength. In addition, the small concave mirror radius of curvature (RoC) of 6 μm gives rise to micron sized polariton confinement in the hybridised modes, which combined with the narrow polariton linewidths at resonance of 150 μeV , may allow the blockade regime for coupled cavities to be reached.^{10,11}

The shape of the coupled cavities is given by the surface formed from the isophase profile of two Gaussian modes calculated for a cavity length of 3 μm and RoC of 6 μm , separated by a distance d .¹³ A 13×13 array of coupled cavity features was fabricated using focused ion beam (FIB) milling,^{13,14} where d was incrementally reduced from 10 μm to 7.5 μm as shown in the microscope image in Fig. 1(a). Note that open cavities can also be realised using laser machining.^{15–17} The coupled cavity array was then coated with 11 pairs of $\text{SiO}_2/\text{TiO}_2$ quarter-wave stacks. The individual hemispherical cavities of the molecules laterally confine the photonic field with a confining potential that is nearly harmonic giving rise to zero-dimensional cavity eigenstates which can be described by Hermite or Laguerre Gaussian profiles depending on the exact symmetry of the confining potential.^{14,18} The RoC of the single cavity concave feature of 6 μm gives an expected Gaussian beam waist of the fundamental mode at the QW position of around 0.89 μm .¹⁸ In the

^{a)}Electronic mail: f.li@sheffield.ac.uk

^{b)}Electronic mail: d.krizhanovskii@sheffield.ac.uk

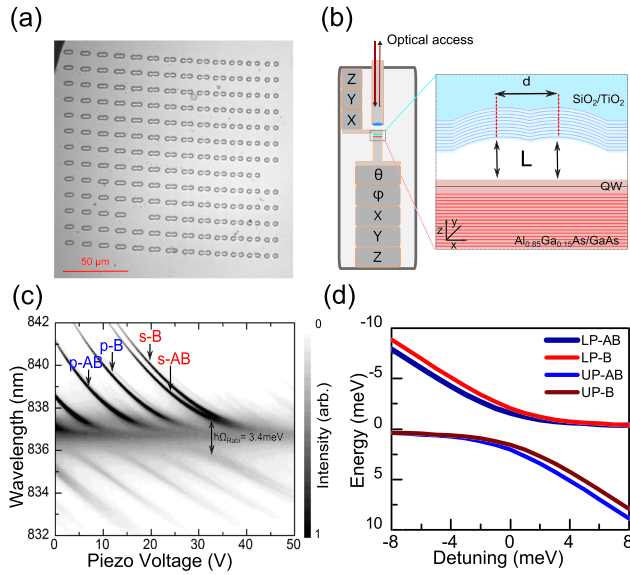


FIG. 1. (a) Microscope image of the coupled cavity array. (b) Schematic of the configuration of the tunable cavity system. (c) Avoided crossing when the cavity is tuned through resonance with the QW exciton. (d) Calculated eigenstates of lower (LP) and upper (UP) polaritons with $J = 1$ meV and $\Omega_{Rabi} = 3.4$ meV.

coupled cavity system studied here, the longitudinal and higher order transverse Gaussian modes in adjacent cavities couple, giving rise to hybridisation of these eigenmodes into various bonding and antibonding eigenstates. The work presented here focuses on the characterisation of the cavities with nominal separations of $7.9 \mu\text{m} < d < 8.26 \mu\text{m}$ where modal coupling of the longitudinal modes of the constituent cavities occurs. The planar semiconductor mirror consists of a 31 pair $\text{Al}_{0.85}\text{Ga}_{0.15}\text{As}/\text{GaAs}$ DBR with a single 10 nm $\text{In}_{0.04}\text{Ga}_{0.96}\text{As}$ QW at an electric-field antinode in a GaAs cavity region, grown via molecular beam epitaxy. The formed cavity structure is shown in Fig. 1(b) where independent xyz-positioning of the two mirrors and angular tilting can be performed *in-situ* using nanopositioners. The tuning range of the goniometer stages is $-3.3^\circ \leq \theta \leq 3.3^\circ$ and $-2.7^\circ \leq \phi \leq 2.7^\circ$ with a minimum step size of 0.02 millidegree. Characterisation of the QW can be performed by moving the top DBR sample out of the optical path revealing an inhomogeneously broadened exciton line-width of $650 \mu\text{eV}$ at low power.

Photoluminescence (PL) spectroscopy of the polaritonic molecules was performed in a homemade bath cryostat at 4 K. Both non-resonant excitation at 630 nm and collection are performed through a custom housed objective lens above the open cavity. The excitation spot diameter was around $10 \mu\text{m}$ with a power of $20 \mu\text{W}$. Using the z-nanopositioner to raise the bottom semiconductor mirror and goniometer stages to achieve a high degree of parallelism between top and bottom mirrors, a mirror separation of $3\lambda/2$ could be reached from an initial separation of > 1 mm. Fine tuning of the cavity mode energies was then performed by applying a DC voltage to the bottom z-nanopositioner which reduces the mirror separation with sub-nm precision. Fig. 1(c) shows the spectra of a typical polaritonic molecule as a function of z-nanopositioner voltage when the lowest energy eigenmodes are tuned through resonance with the QW exciton. Here

the polaritonic molecule has a centre-to-centre distance of $8.08 \mu\text{m}$ and a linear polariser was used to select modes polarised along the long axis of the molecule. The four labelled spectral resonances correspond to the symmetric/antisymmetric modes which arise from coupling of the individual cavity ground states (s-B/s-AB) and the first transverse modes (p-B/p-AB) as discussed below. A distinct anti-crossing is observed between all eigenmodes and the QW exciton with clear lower and upper polariton branches with a Rabi splitting of 3.4 meV. The B/AB modes of the polaritonic molecule system can be described by a 4-level coupled-oscillator model with the Hamiltonian

$$H = \begin{pmatrix} E_X & \Omega_{Rabi}/2 & 0 & 0 \\ \Omega_{Rabi}/2 & E_{c1} & J/2 & 0 \\ 0 & J/2 & E_{c2} & \Omega_{Rabi}/2 \\ 0 & 0 & \Omega_{Rabi}/2 & E_X \end{pmatrix} \quad (1)$$

in which E_X , E_{c1} , and E_{c2} are the energies of the bare exciton and cavity modes, Ω_{Rabi} is the exciton-photon coupling, and J is the cavity-cavity coupling strength. The eigenenergies that describe the upper (UP) and lower (LP) polariton states are given by diagonalising the Hamiltonian of Eq. (1)

$$E_{UP/LP} = \frac{2E_X + (\Delta \pm J/2)}{2} \pm \frac{1}{2} \sqrt{(\Delta \pm J/2)^2 + \Omega_{Rabi}^2}, \quad (2)$$

where Δ is the exciton-photon detuning given by $E_c - E_X$, where we have assumed the cavities are in resonance ($E_c = E_{c1} = E_{c2}$). The calculated eigenenergies as a function of detuning, plotted in Fig. 1(d), exhibit a reduction in the coupling strength (B-AB splitting) as the detuning is tuned to zero due to the coexistence of light-matter and light-light couplings. We observe this reduction experimentally in Fig. 1(c), with a B-AB splitting of ~ 1 meV at large negative detunings, which gradually diminishes when approaching the exciton energy. Since the B-AB splitting between polaritons is contributed by their photonic component increasing the excitonic component leads to reduced photonic coupling and a smaller B-AB splitting.

Real space images of the s-B and s-AB modes shown in Fig. 2(a) clearly exhibit the symmetric and antisymmetric nature of the mode profiles. Note that the parameter d only determines the nominal separation between the overlapping isophase Gaussian profiles of the constituent cavities which define the fabricated coupled cavity shape. The actual mode position is determined by the photonic potential induced from this shape and leads to a modal structure of the coupled cavities with lateral sizes much smaller than the nominal separation.¹³ For example, the s-AB mode in Fig. 2(a) has a nominal separation of $8.0 \mu\text{m}$, whereas in the experiment the measured separation between mode maxima is $2.96 \mu\text{m}$ with full width half maxima of $1.3 \mu\text{m}$. The lateral extent of the higher order modes is typically larger for increasing transverse numbers leading to stronger modal overlap between these modes in coupled cavities. This leads to much higher B-AB splittings in comparison to the ground state coupled s-type modes in the same photonic molecule. As an example, these B-AB modes with higher transverse orders are shown in Figs. 2(b)–2(d), respectively.

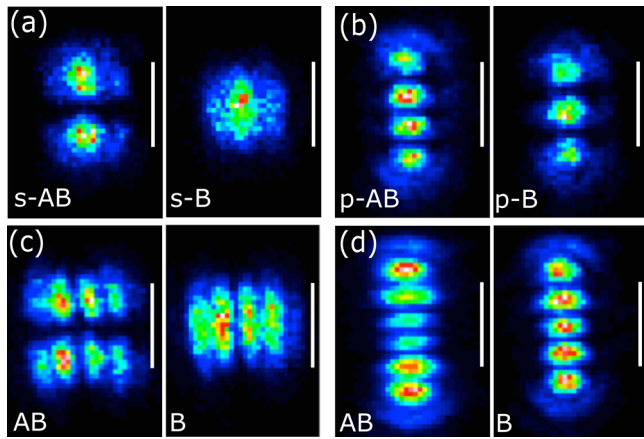


FIG. 2. Tomographic images of the first four pairs of bonding/antibonding states. (a) s-AB/s-B modes ground state mode coupling (b) p-AB/p-B modes due to first transverse mode coupling. (c) AB/B modes due second transverse mode coupling. (d) AB/B modes due to third transverse mode coupling. The scale bar is $4 \mu\text{m}$.

A typical PL spectrum at large negative detuning is shown in Fig. 3(a). Due to the elongated geometry (compared to circular-shaped cavities) of the photonic molecule and the TE-TM splitting induced by the DBR surfaces, we observe two orthogonally linearly polarised sets of s-B and s-AB modes. Fig. 3(b) shows the s-B state at a negative detuning of -9.6 meV . A Lorentzian fit yields a linewidth of $47 \mu\text{eV}$ corresponding to a photonic Q-factor of around 31 500. This is most likely limited by the stability of the system to low frequency acoustic vibrations.¹⁶ Fig. 3(c) shows the lower polariton s-B and s-AB states at zero exciton-photon detuning. Fitting the lower polariton s-B state reveals

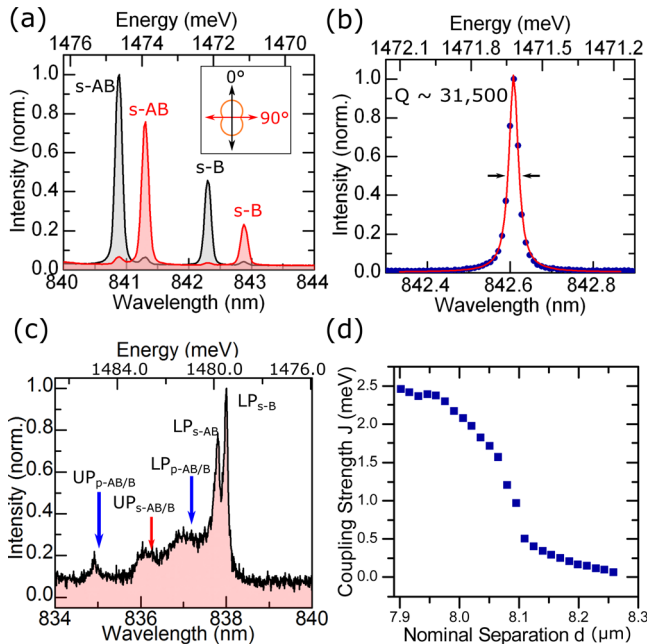


FIG. 3. (a) PL spectrum of the coupled cavity emission at large negative exciton-photon detuning showing orthogonally polarised B-AB doublets. Inset defines the 0° along the long axis of the molecule. (b) s-B mode at negative detuning of $\Delta = -9.6 \text{ meV}$. A Lorentzian fit gives a linewidth of 26.75 pm ($47 \mu\text{eV}$) corresponding to a photonic Q-factor of 31 500. (c) Spectrum at resonance where the s-B polariton has a linewidth of $150 \mu\text{eV}$. (d) The coupling strength J as a function of nominal separation at large negative detuning.

a linewidth of $150 \mu\text{eV}$ which is limited by the inhomogeneously broadened exciton linewidth of $650 \mu\text{eV}$. Narrower polariton resonances can be expected for a semiconductor half cavity containing a narrower linewidth QW.

The coupling strength of the coupled longitudinal modes is plotted against nominal centre-to-centre distance in Fig. 3(d). The transition between uncoupled and coupled cavities occurs abruptly when the centre-to-centre distance is smaller than around $8.1 \mu\text{m}$. At a centre-to-centre distance of $8.26 \mu\text{m}$, we measure a coupling strength of $63 \mu\text{eV}$ which increases continuously to 2.45 meV at $d = 7.90 \mu\text{m}$. Hence the precise control of the coupled cavity separation provided by the FIB milling fabrication process allows the selection of any arbitrary coupling strength between these ranges.

The ability to manipulate the relative angle between top and bottom mirrors *in-situ* using goniometer nanopositioners provides a further degree of freedom to tune the B-AB splitting. This provides high flexibility in choosing the cavity-cavity detuning $\delta = E_{c1} - E_{c2}$ constituting a distinct advantage of open cavities. Furthermore, this allows for the correction of any fabrication imperfections which can cause slight detunings between adjacent cavities even when the planar areas of the mirrors are parallel. The detuning dependent B-AB splitting for coupled cavities is characterized by

$$\Delta E = E_{AB} - E_B = \sqrt{\delta^2 + J^2}. \quad (3)$$

In the experiment, tilting the mirrors tunes δ , allowing to “decouple” the photonic molecule by reaching a $|\delta|$ large enough to significantly reduce the tunnelling probability. Fig. 4(a) displays the spatial profiles of the modes corresponding to the configuration in the panels above. At zero-angle where $\delta = 0$ (middle panel), the polaritonic molecule exhibits s-B and s-AB modes each of which fills both cavities symmetrically, whereas at large negative (left panel)

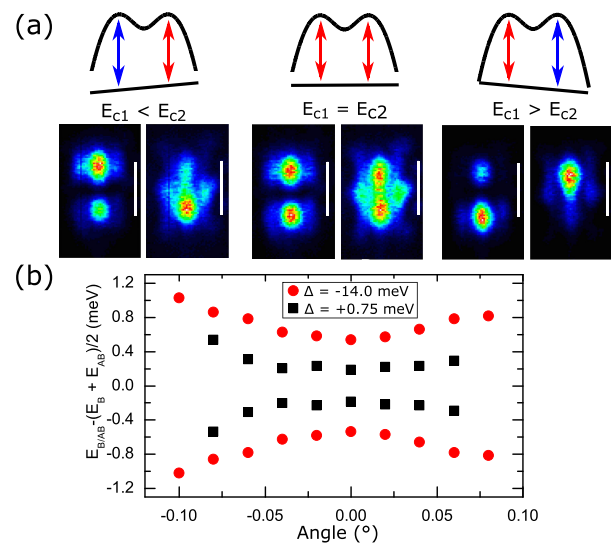


FIG. 4. (a) Real space images of ground state modes at an angle of -0.1° (left panel), at resonance (middle panel), and at an angle of $+0.1^\circ$. The scale bar is $4 \mu\text{m}$. (b) Anticrossing between the s-type cavity eigenmodes when tuned through resonance by varying the angle, and hence cavity-cavity detuning. The red (black) points correspond to $\Delta = -14.0 \text{ meV}$ ($\Delta = +0.75 \text{ meV}$). $\theta = 0^\circ$ is defined at $\delta = 0$.

and positive (right panel) angles, the cavities begin to “decouple” and the modes are more localized in each individual cavity. The B-AB mode splittings are plotted as a function of the relative angle for two exciton-photon detunings corresponding to photonic ($\Delta = -14.0$ meV) and excitonic cases ($\Delta = +0.75$ meV) in Fig. 4(b). For both cases, there is clear anti-crossing behaviour due to the strong cavity-cavity coupling, but the B-AB splitting is greater for the photonic-like case at all angles due to the smaller exciton fraction. The reduction from 1.07 meV at $\Delta = -14.0$ meV to 0.37 meV at $\Delta = +0.75$ meV is consistent with a reduction in the photonic component from 99.6% to 27.6% and is complementary to the tuning by the z-nanopositioner in Fig. 1(c).

In summary, we present polaritonic molecules with full tunability of the cavity-cavity coupling strength through controlled fabrication of the centre-to-centre distance combined with *in-situ* tunability of the exciton-photon and cavity-cavity detunings. This tunability is likely to find a number of applications. First, it may allow the coupling of both the exciton and biexciton line of a pre-selected single QD to the optical modes of the photonic molecule in an efficient manner leading to bright source of entangled photon pairs.¹⁹ Second, the system exhibits excellent potential to observe polariton blockade in coupled cavities where we demonstrate a number of prerequisite conditions such as experimentally observable cavity-cavity tunnelling times (>2 ps), micron sized confinement, and narrow polariton linewidths.^{9–11} For optimum antibunched emission, we estimate a required non-linearity of $U \sim 5$ μ eV using the experimentally measured parameters of $\gamma_{LP} = 150$ μ eV for the ground state bonding mode and $J = 0.5$ meV. In this system, the nonlinearity is manifested as the repulsive polariton-polariton interaction which is inherited from the excitonic component.²⁰ The required value is comparable to the nonlinear polariton-polariton interaction measured in 10 μ m micropillars,²¹ which is expected to be larger in open cavity systems due to the increased lateral confinement.

This work has been supported by the EPSRC Programme Grant No. EP/J007544, ERC Advanced

Investigator Grant EXCIPOL and by the Leverhulme Trust.

- ¹M. Bayer, T. Gutbrod, J. P. Reithmaier, A. Forchel, T. L. Reinecke, P. A. Knipp, A. A. Dremin, and V. D. Kulakovskii, *Phys. Rev. Lett.* **81**, 2582 (1998).
- ²S. Michaelis de Vasconcellos, A. Calvar, A. Dousse, J. Suffczynski, N. Dupuis, A. Lemaître, I. Sagnes, J. Bloch, P. Voisin, and P. Senellart, *Appl. Phys. Lett.* **99**, 101103 (2011).
- ³A. R. A. Chalcraft, S. Lam, B. D. Jones, D. Szymanski, R. Oulton, A. C. T. Thijssen, M. S. Skolnick, D. M. Whittaker, T. F. Krauss, and A. M. Fox, *Opt. Express* **19**, 5670 (2011).
- ⁴S. Ishii and T. Baba, *Appl. Phys. Lett.* **87**, 181102 (2005).
- ⁵A. Armitage, M. S. Skolnick, V. N. Astratov, D. M. Whittaker, G. Panzarini, L. C. Andreani, T. A. Fisher, J. S. Roberts, A. V. Kavokin, M. A. Kaliteevski, and M. R. Vladimirova, *Phys. Rev. B* **57**, 14877 (1998).
- ⁶T. Jacqmin, I. Carusotto, I. Sagnes, M. Abbarchi, D. D. Solnyshkov, G. Malpuech, E. Galopin, A. Lemaître, J. Bloch, and A. Amo, *Phys. Rev. Lett.* **112**, 116402 (2014).
- ⁷A. Dousse, J. Suffczynski, A. Beveratos, O. Krebs, A. Lemaître, I. Sagnes, J. Bloch, P. Voisin, and P. Senellart, *Nature* **466**, 217 (2010).
- ⁸M. Abbarchi, A. Amo, V. Sala, D. Solnyshkov, H. Flayac, L. Ferrier, I. Sagnes, E. Galopin, A. Lemaître, G. Malpuech, and J. Bloch, *Nat. Phys.* **9**, 275 (2013).
- ⁹A. Verger, C. Ciuti, and I. Carusotto, *Phys. Rev. B* **73**, 193306 (2006).
- ¹⁰T. C. H. Liew and V. Savona, *Phys. Rev. Lett.* **104**, 183601 (2010).
- ¹¹M. Bamba, A. Imamoglu, I. Carusotto, and C. Ciuti, *Phys. Rev. A* **83**, 021802 (2011).
- ¹²S. Reitzenstein, N. Gregersen, C. Kistner, M. Strauss, C. Schneider, L. Pan, T. R. Nielsen, S. Höfling, J. Mørk, and A. Forchel, *Appl. Phys. Lett.* **94**, 061108 (2009).
- ¹³L. Flatten, A. Trichet, and J. Smith, “Spectral engineering of coupled open-access microcavities,” e-print [arXiv:1503.07687v1](https://arxiv.org/abs/1503.07687v1).
- ¹⁴A. A. P. Trichet, P. R. Dolan, D. M. Coles, G. M. Hughes, and J. M. Smith, *Opt. Express* **23**, 17205 (2015).
- ¹⁵A. Muller, E. B. Flagg, J. R. Lawall, and G. S. Solomon, *Opt. Lett.* **35**, 2293 (2010).
- ¹⁶L. Greuter, S. Starosielec, D. Najer, A. Ludwig, L. Duempelmann, D. Rohner, and R. J. Warburton, *Appl. Phys. Lett.* **105**, 121105 (2014).
- ¹⁷J. Benedikter, T. Hümmer, M. Mader, B. Schleder, J. Reichel, T. W. Hänsch, and D. Hunger, *New J. Phys.* **17**, 053051 (2015).
- ¹⁸S. Dufferwiel, F. Fras, A. Trichet, P. M. Walker, F. Li, L. Giriunas, M. N. Makhonin, L. R. Wilson, J. M. Smith, E. Clarke, M. S. Skolnick, and D. N. Krizhanovskii, *Appl. Phys. Lett.* **104**, 192107 (2014).
- ¹⁹A. Dousse, J. Suffczynski, O. Krebs, A. Beveratos, A. Lemaître, I. Sagnes, J. Bloch, P. Voisin, and P. Senellart, *Appl. Phys. Lett.* **97**, 081104 (2010).
- ²⁰C. Ciuti, V. Savona, C. Piermarocchi, A. Quattropani, and P. Schwendimann, *Phys. Rev. B* **58**, 7926 (1998).
- ²¹L. Ferrier, E. Wertz, R. Johné, D. D. Solnyshkov, P. Senellart, I. Sagnes, A. Lemaître, G. Malpuech, and J. Bloch, *Phys. Rev. Lett.* **106**, 126401 (2011).